

Time-Domain *Ab Initio* Simulation of Electron and Hole Relaxation Dynamics in a Single-Wall Semiconducting Carbon Nanotube

Bradley F. Habenicht, Colleen F. Craig, and Oleg V. Prezhdo*

Department of Chemistry, University of Washington, Seattle, Washington 98195-1700, USA

(Received 13 October 2005; published 11 May 2006)

The electron and hole relaxation in the (7, 0) zigzag carbon nanotube is simulated in time domain using a surface-hopping Kohn-Sham density functional theory. Following a photoexcitation between the second van Hove singularities, the electrons and holes decay to the Fermi level on characteristic subpicosecond time scales. Surprisingly, despite a lower density of states, the electrons relax faster than the holes. The relaxation is primarily mediated by the high-frequency longitudinal optical (LO) phonons. Hole dynamics are more complex than the electron dynamics: in addition to the LO phonons, holes couple to lower frequency breathing modes and decay over multiple time scales.

DOI: [10.1103/PhysRevLett.96.187401](https://doi.org/10.1103/PhysRevLett.96.187401)

PACS numbers: 78.67.Ch, 03.65.Sq, 31.10.+z, 73.22.-f

The unique structural, mechanical, and electronic properties of carbon nanotubes (CNT) [1] have suggested a variety of applications including nanoscale logic gates [2], antennas [3], conductance switches [4], quantum wires [5], and field-effect transistors [6]. Spectroscopic techniques now permit the characterization of nanotube diameters, chiralities [7], and nanotube-nanotube interactions [8], affording more insight into the unique nature of these structures. While these experimental breakthroughs have enabled an unprecedented level of observational detail, specific knowledge of the electron and phonon dynamics in CNTs is becoming increasingly important. For instance, charge-phonon interaction directly affects conductivity and energy loss in CNT wires [5] and field-effect transistors [6], and provides a mechanism for the observed superconductivity of CNTs [9]. Further, detailed information on electron and hole relaxation is pivotal to such applications as CNT logic gates [2] and optical switches [4]. As research and device fabrication move forward, a clear understanding of these processes is critical to the development of novel materials whose response is directly related to such dynamics.

Numerous time-resolved experiments have revealed intriguing and controversial features of electron-phonon relaxation in CNTs in response to external stimuli [10–17]. Depending on sample preparation, excitation energy, light intensity, and detection technique, the relaxation dynamics range from 100 fs or less [11,13,15], to hundreds of femtoseconds [10,12,17], to more than a picosecond [16]. The electron-hole annihilation takes an order of magnitude longer than the intraband relaxation. The relaxation is slower in isolated CNTs than in CNT bundles and CNT-polymer mixtures, where tube-tube and tube-matrix interactions provide additional decay channels. The relaxation is faster in larger CNTs, since they have greater densities of state (DOS), which also causes a more rapid decay of higher energy excitations [10,17]. The participation of both low frequency radial-breathing modes (RBM) and high-frequency longitudinal optical (LO) *G*

phonons in the charge carrier relaxation has been detected [11,18,19]. A thorough understanding and interpretation of the experimental data requires detailed modeling of the observed phenomena at the atomic level.

The current letter presents the first time-domain *ab initio* simulation of the electron and hole dynamics in a CNT. The simulated dynamics agree with experimental time scales, establish the electron and hole relaxation pathways, characterize the electronic states and phonon modes that facilitate energy dissipation, and expose a number of surprising aspects of the relaxation process. In particular, the simulation shows for the (7, 0) nanotube that the holes relax more slowly between the sub-bands than the electrons, even though the holes possess a denser manifold of states. The electrons decay by a single exponential, while the holes exhibit first a Gaussian and later an exponential decay component. Relaxation of both electrons and holes is most strongly promoted by the C-C stretching *G* phonons with frequencies around 1500 cm⁻¹. In contrast to electrons, holes also couple to the lower frequency breathing modes.

While a number of state-of-the-art *ab initio* calculations of the electronic structure of CNTs are available in the literature [20], and tight-binding molecular dynamics (MD) simulations of CNT response to laser excitations have been reported [21], this is the first *ab initio* non-adiabatic (NA) MD study of the electron-phonon relaxation in a photoexcited nanotube. The study is made possible by the recent implementation [22] of the fewest-switches surface-hopping (FSSH) approach [23,24] within the framework of the time-dependent (TD) Kohn-Sham (KS) theory. Traditional Ehrenfest-TDKS theory cannot describe equilibration and electron-phonon energy exchange [25,26]. FSSH-TDKS, however, is a stochastic approach that satisfies detailed balance [23] and can be viewed as a master equation with TD transition rates [26] that give a proper account of the short-time dynamics [27].

The TDKS theory used here is a quasiparticle formalism that focuses on charge-phonon interactions. Quasiparticle

formalisms can successfully predict many electronic properties of CNTs, including optical transitions [20]. They are particularly suitable for describing the dynamics of hot electron-hole pairs, which are created when the photoexcited state scatters into the electron-hole continuum [13,17,28]. This process ultimately results in phonon emission and relaxation of the excited state. The electron-hole correlations—manifested in CNTs by excitonic signatures in the optical properties [12,29]—are implicitly included in the TDKS approach through the exchange-correlation functional and the dependence of the electron density on hole and electron occupations.

The smallest semiconducting zigzag (7, 0) CNT [1] with diameter 5.5 Å has been chosen to minimize the size of the electronic basis and simulation cell. The simulations are performed in VASP [30], augmented with the FSSH-TDKS functionality [22]. The Perdew-Wang generalized gradient approximation (GGA) [31], Vanderbilt ultrasoft pseudopotentials [32], periodic boundary conditions, and converged plane-wave basis sets are employed. Constructing the simulation cell [33] from four CNT unit cells and 112 carbon atoms (see Fig. 1) expands the available phonon spectrum [9]. To prevent spurious interactions between the images, 8 Å of vacuum are added in the direction perpendicular to the axis of the tube. The structure of the nanotube and the dimension of the simulation cell along the tube are optimized to obtain the minimum energy structure. After heating the system to 300 K by repeated velocity rescaling, a 1.5 ps microcanonical trajectory is run in the ground electronic state with a 1 fs time step, and 400 initial conditions are sampled for the relaxation dynamics.

The KS theory [34] represents the one-electron density of an N -electron system by the sum over KS orbitals $\rho(x, t) = \sum_{a=1}^N |\varphi_a(x, t)|^2$. The orbitals evolve following

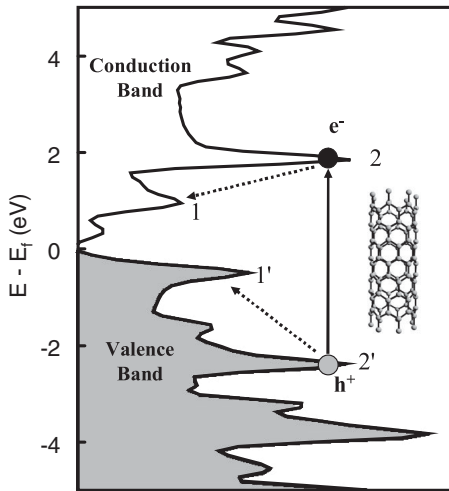


FIG. 1. DOS of the (7, 0) zigzag carbon nanotube (shown in inset). An electron is optically excited between the second van Hove singularities $2' \rightarrow 2$. The electron and hole then decay to the first singularities $1'$ and 1 on a subpicosecond time scale.

the Dirac TD variational principle [35] by the single-particle Schrödinger equations

$$i\hbar \frac{\partial \varphi_a(x, t)}{\partial t} = H[\varphi(x, t), \mathbf{R}(t)]\varphi_a(x, t), \quad a = 1, \dots, N \quad (1)$$

that are coupled through the orbital dependence of the functional H . The functional is explicitly TD due to the evolution of the ions $\mathbf{R}(t)$. The TDKS Eqs. (1) are solved in the basis of adiabatic KS orbitals that are solutions to the time-independent KS problem $H\psi_j(x, \mathbf{R}) = \epsilon_j(\mathbf{R})\psi_j(x, \mathbf{R})$. The many-electron state is represented by a Slater determinant (SD) formed with $\varphi(x, t)$. The SD evolves due to ionic motion into a superposition of adiabatic SDs

$$|\varphi_a \cdots \varphi_c\rangle = \sum_{j \neq \dots \neq l}^N C_{j \dots l}(t) |\psi_j \cdots \psi_l\rangle. \quad (2)$$

The expansion coefficients in the superposition obey

$$i\hbar \frac{\partial C_{j \dots l}(t)}{\partial t} = \sum_{p \neq \dots \neq q}^N C_{p \dots q}(t) [E_{p \dots q} \delta_{jp} \cdots \delta_{lq} + \mathbf{D}_{j \dots l; p \dots q} \cdot \dot{\mathbf{R}}], \quad (3)$$

where $\mathbf{D}_{j \dots l; p \dots q} = -i\hbar \langle \langle \psi_j \cdots \psi_l | \nabla_{\mathbf{R}} | \psi_p \cdots \psi_q \rangle \rangle$ is the NA coupling vector. FSSH uses the coefficients and the NA coupling to define the transition probabilities between the adiabatic states [24]

$$dP_{j \dots l; m \dots n} = \frac{-2 \operatorname{Re}(A_{j \dots l; m \dots n}^* \mathbf{D}_{j \dots l; m \dots n} \cdot \dot{\mathbf{R}})}{A_{j \dots l; m \dots n}} dt; \quad (4)$$

$$A_{j \dots l; m \dots n} = C_{j \dots l} C_{m \dots n}^*$$

Should the calculated probability be negative, it is set to zero. The transition probabilities are computed on the fly for the current ionic configuration. The rates are zero initially, which is essential for the short-time dynamics that are quadratic in time, as manifested in the quantum Zeno effect [27]. Equations (1)–(4) are propagated with a 10^{-3} fs time step. Further details of the simulation protocol will be reported elsewhere.

The electron and hole relaxation under investigation is initiated by an excitation from the second vHs below the Fermi level to the second vHs above the Fermi level (Fig. 1), as in the recent ultrafast laser experiments [12,15]. The states within the singularities are chosen based on the strongest transition dipole moment at a given initial time. Over a third of all excitations occur between two pairs of electron and hole states. The electrons and holes relax nonadiabatically through the first vHs above and below the Fermi level to their corresponding band edges.

Figure 2 details the electron and hole relaxation dynamics. Figure 2(a) shows the total population of the states within the second vHs, as defined by the dashed lines in

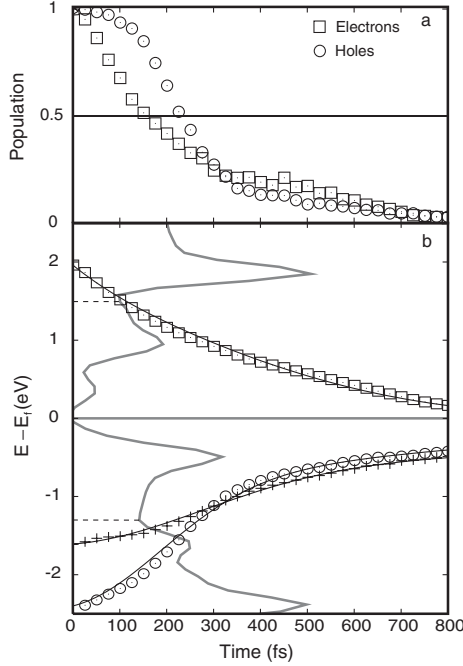


FIG. 2. Electron and hole relaxation dynamics. (a) The populations of the second singularities, as defined by the dashed lines in part (b), decay slower for the holes than the electrons in spite of the higher hole DOS. (b) The average energies of electrons and holes are fitted by a sum of Gaussian and exponential components (solid lines) with the fit parameters defined in Eq. (5) and presented in Table I. Holes starting closer to the Fermi energy (pluses) decay more slowly than holes starting farther from the Fermi energy (circles), in agreement with experiments [10,17].

Fig. 2(b). Over the course of the simulation, the populations transfer from the second to first vHs, with very little contribution from the higher energy states. That the holes decay more slowly than the electrons is quite surprising, since the larger DOS of the holes should facilitate faster relaxation. Figure 2(a) clearly indicates a Gaussian and an exponential component in the hole relaxation. A Gaussian component can hardly be distinguished in the electron relaxation. The average electron and hole energies shown in Fig. 2(b) decay similarly to the populations of Fig. 2(a). In addition to the hole energy decay starting from the main peak within the second vHs (circles), Fig. 2(b) shows the hole energy decay starting from the secondary peak closer to the Fermi energy (pluses). The energy decay is fit with the sum of the Gaussian and exponential components

$$|E - E_f|(t) = |E - E_f|(0)[Ae^{-t/\tau_e} + (1 - A)e^{-(t/\tau_g)^2}] \quad (5)$$

with the fitting parameters listed in Table I. The exponential component dominates the electron decay. Holes show both Gaussian and exponential decay. The Gaussian relaxation observed with holes at short times is associated with coherent quantum dynamics [27] that results in delocalization of holes over their dense state manifold. The lower density of electronic states restricts the amplitude of

TABLE I. Parameters of the Gaussian plus exponential fits (5) of the electron and hole energy decays, Fig. 2(b).

Data set	τ_g , fs	τ_e , fs	A
e^- (squares)	200	320	0.80
e^- (squares) ^a	...	380	1.00
h^+ (circles)	280	710	0.35
h^+ (pluses)	410	940	0.45

^aThe purely exponential fit line [not shown in Fig. 2(b)] is very close to the Gaussian plus exponential fit.

the coherent dynamics. Holes starting closer to the Fermi energy have smaller DOS and relax more slowly, in agreement with the experimental data [10,17].

The two-component hole decay is promoted by strong coupling of holes to both high and lower frequency phonons, Fig. 3. In contrast, electrons interact more strongly with the high-frequency modes. The Fourier transforms of the energies of the two most optically active electron and hole state pairs shown in Fig. 3 were computed from the microcanonical trajectory that was used to sample the photoexcited states for the NA dynamics. The *G*-type longitudinal optical (LO) phonons with frequencies around 1500 cm^{-1} provide the fastest relaxation pathway for both electrons and holes. The stronger coupling of the holes to

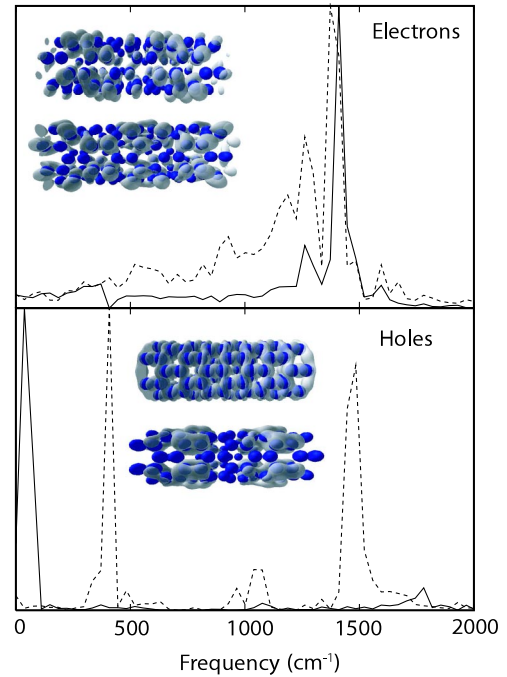


FIG. 3 (color online). Fourier transforms of the energies of the two most optically active electron and hole states, top and bottom panels, respectively. The state charge densities are shown in the insets. The solid and dashed lines correspond to the lower and upper density images, respectively. The electron relaxation is facilitated by the C-C stretching LO phonons around 1500 cm^{-1} . The holes relax through both the LO modes and the low frequency breathing modes below 500 cm^{-1} .

the radial-breathing modes (RBM) at frequencies below 500 cm^{-1} can be rationalized by the better match between the nodal structures of the hole states and RBMs. The lower energy valence band (VB) states that support holes have fewer nodes than the conduction band states that support electrons; similarly, RBMs have fewer nodes than LO phonons. As a result, RBMs couple better to the VB states. The stronger coupling to the lower frequency RBMs explains why the hole relaxation is slower than the electron relaxation, even though holes have a higher DOS. The coupling of holes to lower frequency modes may also contribute to the slowing of the hole dynamics in quantum dots, where impact ionization gives multiple electron-hole pairs upon absorption of a single photon [36].

The time scales for the electron and hole relaxation computed for the (7, 0) tube are within the range of the ultrafast spectroscopy data [10–17]. The calculations support the picture where the photoexcited state scatters into the continuum of hot electron and hole pairs, which relax by phonon emission [13,28]. The involvement of RBM in the CNT charge carrier dynamics seen in our simulation has been detected by both current or voltage [18] and spectroscopic [11] measurements. The coupling of the electronic system to the LO phonons has been detected in the Raman spectra [19]. The reported *ab initio* NA dynamics also agree with the tight-binding electronic structure calculations, in which the electron-phonon scattering was dominated by the RBM and LO phonons in two narrow frequency regions [37]. Our previous studies of solvated electrons [38] and molecule-semiconductor interfaces [39] also indicated that high-frequency vibrations are very effective in promoting charge transfer and relaxation.

In summary, we have investigated the electron and hole relaxation dynamics in the (7, 0) semiconducting CNT by performing a time-domain atomistic *ab initio* NA dynamics simulation for the first time. Our results agree with the experimental data and provide valuable insights into the relaxation mechanisms. The key observations include the slower, multiple time scale hole relaxation compared to the faster single exponential electron dynamics, despite the smaller electronic DOS, the increase of the relaxation rate with excitation energy, the dominant role of high-frequency LO phonons, and the substantial contribution of RBM to hole, but not electron, relaxation.

The authors are grateful to Dr. Dmitri Kilin, Dr. Kiril Tsemekhman, Dr. Sergei Tretiak, and Ms. Svetlana Kilina for fruitful discussions. The research was supported by Grants from DOE No. DE-FG02-05ER15755 and ACS PRF No. 41436-AC6.

*Corresponding author.

Email address: prezhdo@u.washington.edu

- [1] R. Saito, G. Dresselhaus, and M. S. Dresselhaus, *Physical Properties of Carbon Nanotubes* (Imperial College Press, London, 1998).

- [2] N. Mason *et al.*, *Science* **303**, 655 (2004).
 [3] M. S. Dresselhaus, *Nature (London)* **432**, 959 (2004).
 [4] Y.-C. Chen *et al.*, *Appl. Phys. Lett.* **81**, 975 (2002).
 [5] S. J. Tans *et al.*, *Nature (London)* **386**, 474 (1997).
 [6] J. A. Misewich *et al.*, *Science* **300**, 783 (2003).
 [7] S. M. Bachilo *et al.*, *Science* **298**, 2361 (2002).
 [8] M. Y. Sfeir *et al.*, *Science* **306**, 1540 (2004).
 [9] K. P. Bohnen *et al.*, *Phys. Rev. Lett.* **93**, 245501 (2004).
 [10] T. Hertel and G. Moos, *Phys. Rev. Lett.* **84**, 5002 (2000).
 [11] H. Htoon *et al.*, *Phys. Rev. Lett.* **94**, 127403 (2005).
 [12] O. J. Korovyanko *et al.*, *Phys. Rev. Lett.* **92**, 017403 (2004).
 [13] G. Lanzani *et al.*, *Synth. Met.* **155**, 246 (2005).
 [14] Y. Z. Ma *et al.*, *Phys. Rev. Lett.* **94**, 157402 (2005).
 [15] C. Manzoni *et al.*, *Phys. Rev. Lett.* **94**, 207401 (2005); L. Huang and T. D. Krauss, *Phys. Rev. Lett.* **96**, 057407 (2006).
 [16] G. N. Ostojic *et al.*, *Phys. Rev. Lett.* **92**, 117402 (2004); F. Wang *et al.*, *Phys. Rev. Lett.* **92**, 177401 (2004).
 [17] M. Zamkov *et al.*, *Phys. Rev. Lett.* **94**, 056803 (2005).
 [18] B. J. LeRoy *et al.*, *Nature (London)* **432**, 371 (2004).
 [19] M. Oron-Carl *et al.*, *Nano Lett.* **5**, 1761 (2005).
 [20] V. Barone *et al.*, *Nano Lett.* **5**, 1621 (2005); C. D. Spataru *et al.*, *Phys. Rev. Lett.* **92**, 077402 (2004); Z. Y. Zhou *et al.*, *J. Am. Chem. Soc.* **126**, 3597 (2004).
 [21] T. Dumitrica *et al.*, *Phys. Rev. Lett.* **92**, 117401 (2004); A. H. Romero *et al.*, *Nano Lett.* **5**, 1361 (2005).
 [22] C. F. Craig, W. R. Duncan, and O. V. Prezhdo, *Phys. Rev. Lett.* **95**, 163001 (2005).
 [23] P. V. Parahdekar and J. C. Tully, *J. Chem. Phys.* **122**, 094102 (2005).
 [24] J. C. Tully, *J. Chem. Phys.* **93**, 1061 (1990).
 [25] A. P. Horsfield *et al.*, *J. Phys. Condens. Matter* **16**, 8251 (2004).
 [26] G. Kab, *Phys. Rev. E* **66**, 046117 (2002).
 [27] P. Exner, *J. Phys. A* **38**, L449 (2005); O. V. Prezhdo, *Phys. Rev. Lett.* **85**, 4413 (2000); O. V. Prezhdo and P. J. Rossky, *Phys. Rev. Lett.* **81**, 5294 (1998).
 [28] Y.-Z. Ma *et al.*, *J. Phys. Chem. B* **109**, 15 671 (2005).
 [29] G. Dukovic *et al.*, *Nano Lett.* **5**, 2314 (2005); F. Wang *et al.*, *Science* **308**, 838 (2005).
 [30] G. Kresse and J. Furthmüller, *Comput. Mater. Sci.* **6**, 15 (1996).
 [31] J. P. Perdew, *Electronic Structure of Solids* (Akademie Verlag, Berlin, 1991).
 [32] D. Vanderbilt, *Phys. Rev. B* **41**, 7892 (1990).
 [33] J. T. Frey and D. J. Doren, *TubeGen 3.3* (University of Delaware, Newark, DE, 2005).
 [34] W. Kohn and L. J. Sham, *Phys. Rev.* **140**, A1133 (1965).
 [35] M. A. L. Marques and E. K. U. Gross, *Annu. Rev. Phys. Chem.* **55**, 427 (2004).
 [36] R. J. Ellingson *et al.*, *Nano Lett.* **5**, 865 (2005); R. D. Schaller and V. I. Klimov, *Phys. Rev. Lett.* **92**, 186601 (2004).
 [37] V. Perebeinos *et al.*, *Phys. Rev. Lett.* **94**, 027402 (2005); **94**, 086802 (2005).
 [38] O. V. Prezhdo and P. J. Rossky, *J. Phys. Chem.* **100**, 17 094 (1996).
 [39] W. R. Duncan, W. M. Stier, and O. V. Prezhdo, *J. Am. Chem. Soc.* **127**, 7941 (2005).